



In Vitro Differential Diagnosis of Clavus and Verruca by a Predictive Model Generated from Electrical Impedance

Chien-Ya Hung¹, Pei-Lun Sun², Shu-Jen Chiang³, Fu-Shan Jaw^{1*}

1 Institute of Biomedical Engineering, National Taiwan University, Taipei, Taiwan, **2** Department of Dermatology, Mackay Memorial Hospital, Taipei, Taiwan, **3** Institute of Zoology, National Taiwan University, Taipei, Taiwan

Abstract

Background: Similar clinical appearances prevent accurate diagnosis of two common skin diseases, clavus and verruca. In this study, electrical impedance is employed as a novel tool to generate a predictive model for differentiating these two diseases.

Materials and Methods: We used 29 clavus and 28 verruca lesions. To obtain impedance parameters, a LCR-meter system was applied to measure capacitance (C), resistance (R_e), impedance magnitude (Z), and phase angle (θ). These values were combined with lesion thickness (d) to characterize the tissue specimens. The results from clavus and verruca were then fitted to a univariate logistic regression model with the generalized estimating equations (GEE) method. In model generation, $\log Z_{SD}$ and θ_{SD} were formulated as predictors by fitting a multiple logistic regression model with the same GEE method. The potential nonlinear effects of covariates were detected by fitting generalized additive models (GAM). Moreover, the model was validated by the goodness-of-fit (GOF) assessments.

Results: Significant mean differences of the index d , R_e , Z , and θ are found between clavus and verruca ($p < 0.001$). A final predictive model is established with Z and θ indices. The model fits the observed data quite well. In GOF evaluation, the area under the receiver operating characteristics (ROC) curve is 0.875 (> 0.7), the adjusted generalized R^2 is 0.512 (> 0.3), and the p value of the Hosmer-Lemeshow GOF test is 0.350 (> 0.05).

Conclusions: This technique promises to provide an approved model for differential diagnosis of clavus and verruca. It could provide a rapid, relatively low-cost, safe and non-invasive screening tool in clinic use.

Citation: Hung C-Y, Sun P-L, Chiang S-J, Jaw F-S (2014) *In Vitro* Differential Diagnosis of Clavus and Verruca by a Predictive Model Generated from Electrical Impedance. PLoS ONE 9(4): e93647. doi:10.1371/journal.pone.0093647

Editor: Johanna M. Brandner, University Hospital Hamburg-Eppendorf, Germany

Received: September 8, 2013; **Accepted:** March 8, 2014; **Published:** April 4, 2014

Copyright: © 2014 Hung et al. This is an open-access article distributed under the terms of the Creative Commons Attribution License, which permits unrestricted use, distribution, and reproduction in any medium, provided the original author and source are credited.

Funding: This study was supported by grants from the National Science Council (NSC 100-2923-E-002-007-MY3, and NSC 101-2221-E-002-016), Taiwan. The funders had no role in study design, data collection and analysis, decision to publish, or preparation of the manuscript.

Competing Interests: The authors have declared that no competing interests exist.

* E-mail: jaw@ntu.edu.tw

Introduction

Verruca and clavus are two skin disorders commonly encountered in dermatological clinics. Verruca, also referred to as wart, is an infection by human papillomaviruses. Based on the involved site and morphology, verruca can be categorized into several clinical forms, such as verruca vulgaris, plantar and palmar warts, verruca plana, anogenital warts, condyloma, etc. [1]. The former two forms are far more common than the others. These two forms are single or multiple keratotic spiny papules or nodules on hands and/or feet. They are symptomless but can cause pain when grow endophytically on soles. Punctate black dots in verruca, which result from thrombosed capillaries, can be observed by dermoscopy. Verruca lesions may increase in size and number with time and can be contagious.

Although verruca and clavus resemble each other in clinical symptoms, appearances and predilection sites, the latter unlike the former is not contagious. Clavus results from prolonged pressure and friction on the skin [2]. Clavus lesions are painful hard keratotic papules and nodules on soles and palms. Under a dermoscope, a clavus has a compact, homogeneous translucent

central core. There may be some hemorrhages resulting from ruptured capillaries due to shearing forces on skin. No punctate black dots are observed in clavus (Figure S1).

Differential diagnosis between verruca and clavus is mainly based on etiology, pathogenesis, treatment, and means of prevention. The standard treatment for verruca is liquid nitrogen cryotherapy. Other therapeutic modalities include curettage, surgical excision, chemical caustics, and immunotherapies. On the other hand, paring of central radix of corn and topical keratolytics are used in treating clavus [1,2]. Histopathology is of great diagnostic value for these two diseases. In typical verruca, there are hyperkeratosis, parakeratosis and acanthosis of epidermis with koilocytes at the upper epidermis and dilated, thrombosed dermal capillaries. As to clavus, there is a prominent parakeratotic plug in the stratum corneum with an underlying atrophied stratum Malpighian layer. Although dermoscopy is a useful non-invasive tool to make the differential diagnosis, its clinical application is operator-dependent, especially in those cases where typical features are lacking. Therefore, finding an effective alternative approach for differentiating between clavus and verruca is highly desirable for clinical diagnosis.

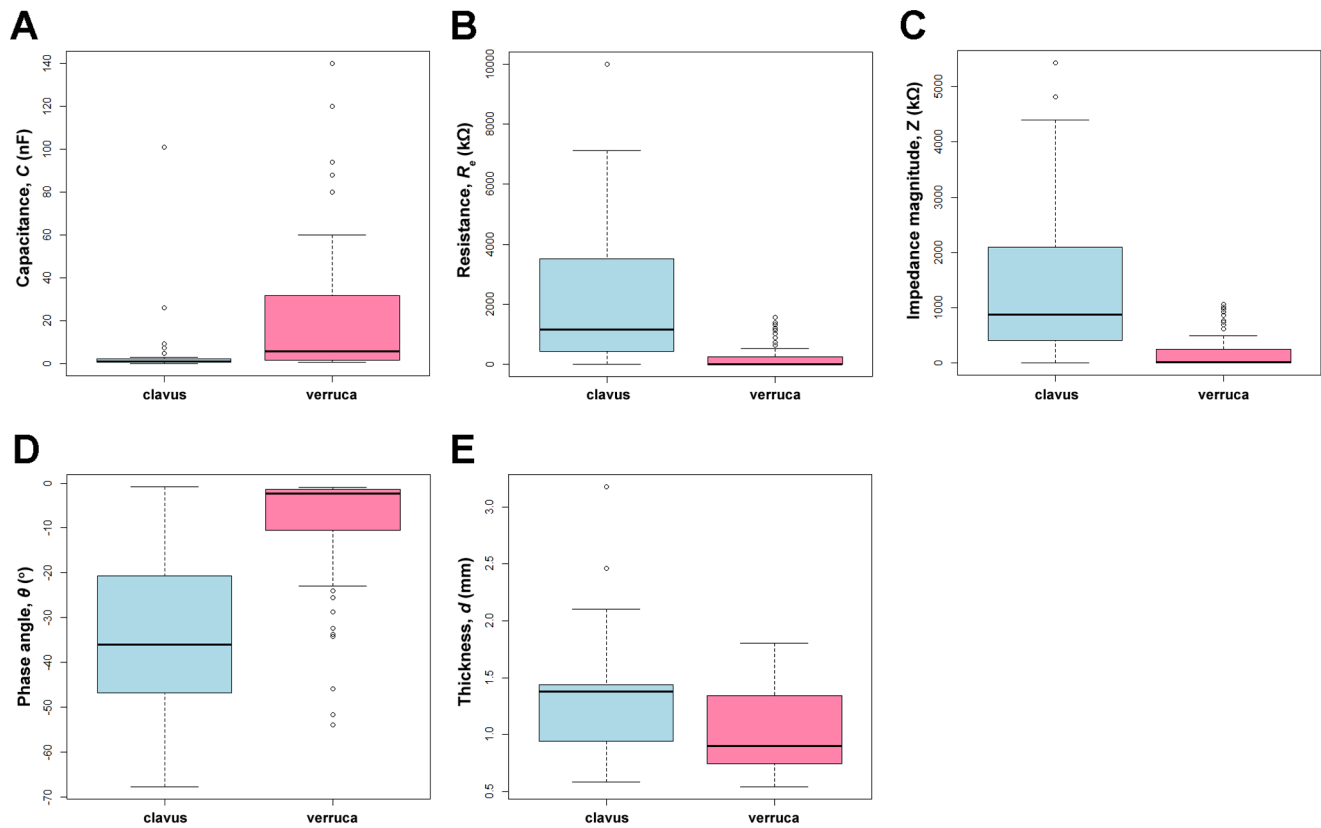


Figure 1. Conditional box plots of the all five measured indices, stratified by clavus and verruca. The lower edge, middle line, and upper edge of the box represent the 25th, 50th, and 75th percentiles of the distribution of the measured index, at 80 Hz. The box plots, A, B, C, D, and E, are for capacitance (C), resistance (R_e), impedance magnitude (Z), phase angle (θ) and thickness (d), respectively.
doi:10.1371/journal.pone.0093647.g001

Electrical impedance, known as a rapid, safe tool with a relatively low cost, has recently been used in measuring skin or stratum corneum hydration [3–12]. It has also been applied to distinguish allergic and irritant contact dermatitis by evaluating the degree of irritation in human skin [13–15]. In addition, the electrical impedance values have been assessed to discriminate skin tumors, such as melanoma, dysplastic nevi, nodular basal cell carcinoma, superficial basal cell carcinoma, as well as benign and malignant skin lesions [16–22]. Clavus has a much thicker stratum corneum and a thinner epidermis than verruca. It is thus expected that their differential thickness and capacitance of stratum corneum will cause differences in their electrical impedance, which can be used as a predictive tool for diagnosing the two types of skin disorders.

In this study, we employed electrical impedance to differentiate between clavus and verruca. The electrical properties of target tissues were measured after a small current or voltage had been applied to them. The resulting impedance values reflected well the different histological constituents of clavus and verruca. It appears quite promising that our study will help build an electrical impedance system for clinical use in the future to quickly and unequivocally discern between clavus and verruca.

Materials and Methods

On the basis of dermoscopic features, specimens were diagnosed and collected by dermatologists from clavus and verruca patients at out-patient clinic. A total of 57 lesions obtained from hands or feet of 29 patients consisted of 29 clavus and 28 verruca lesions.

The criteria for a valid specimen were as follows: Each specimen was (1) diagnosed unequivocally under a dermoscope, (2) greater than 3 mm in diameter, (3) collected from a patient whose lesion has not been treated before, and, (4) regarded as independent if more than one lesion was removed from the same patient. All the samples were processed in accordance with standard treatment protocols for clavus and verruca at our hospital, *i.e.* paring the outer part of the lesions, and applying triacetic acid solution and liquid nitrogen cryotherapy on clavus and verruca, respectively. All the samples were subjected to impedance measuring without any patient information, except the diagnosis. After measuring, all the samples were discarded and disinfected. No patient medical profiles were recorded, thus no linkage between the patients and the samples could be retrieved thereafter.

Impedance measurement

To assemble an electrical impedance system, both sides of each specimen were sealed by two pieces of insulation tape, each with a 3 mm hole in the center. Two holes on each side of the insulation tape were allocated on opposing sides. Therefore, a controlled area of the specimen was used for measurement. This was followed by attaching a pair of pre-gelled electrodes (MEDI-TRACE Mini, Kendall/Tyco, USA) to the two tape holes. Next, the sample was placed in a shielding chamber to reduce noises. Its electrical properties were then measured by a commercial LCR-meter (LCR-821, Instek, Taiwan) under 1 V, at the frequencies of 50 Hz, 80 Hz, 100 Hz, 200 Hz, 1 kHz, 2 kHz, 5 kHz, 10 kHz, 100 kHz, and 1 MHz. The data acquisitions were immediately performed after setup, at 30 min and 60 min. The impedance

Table 1. Comparison of impedance data between clavus and verruca at 80 Hz.

	Clavus	Verruca	Total	<i>p</i> value
Number of subjects	15	14	29	
Number of lesions	29	28	57	
Number of observations	87	84	171	
Measured variable:				
<i>C</i> (nF)	4.21 ± 15.31	19.85 ± 28.66	11.84 ± 24.07	0.099
	1.24 (0.17, 101)	5.85 (0.80, 140)	2.10 (0.17, 140.00)	
<i>R_e</i> (kΩ)	1874.58 ± 2095.43	209.02 ± 397.98	1061.63 ± 1734.63	<0.001
	1153.50 (1.90, 10000)	10.20 (0.74, 1559)	307.50 (0.74, 10000)	
<i>Z</i> (kΩ)	1280.19 ± 1279.58	181.15 ± 311.53	753.70 ± 1094.39	<0.001
	873.90 (2.56, 5436)	16.24 (0.73, 1063)	357.30 (0.73, 5436)	
<i>θ</i> (°)	-33.71 ± 18.36	-8.84 ± 12.69	-21.80 ± 20.16	<0.001
	-36.00 (-67.70, -0.81)	-2.36 (-53.90, -0.99)	-18.30 (-67.70, -0.81)	
<i>d</i> (mm)	1.34 ± 0.55	1.02 ± 0.36	1.19 ± 0.49	<0.001
	1.38 (0.58, 3.18)	0.90 (0.54, 1.80)	1.10 (0.54, 3.18)	
Transformed variable:				
<i>C_{SD}</i>	-0.06 ± 0.85	0.80 ± 1.59	0.36 ± 1.33	0.100
	-0.23 (-0.29, 5.30)	0.03 (-0.25, 7.46)	-0.18 (-0.29, 7.46)	
<i>R_{eSD}</i>	1.11 ± 1.74	-0.27 ± 0.33	0.43 ± 1.44	<0.001
	0.51 (-0.45, 7.85)	-0.44 (-0.45, 0.85)	-0.19 (-0.45, 7.85)	
<i>Z_{SD}</i>	1.13 ± 1.61	-0.26 ± 0.39	0.46 ± 1.38	<0.001
	0.61 (-0.48, 6.35)	-0.46 (-0.48, 0.85)	-0.04 (-0.48, 6.35)	
<i>θ_{SD}</i>	-0.33 ± 0.88	0.87 ± 0.61	0.24 ± 0.97	<0.001
	-0.44 (-1.96, 1.25)	1.18 (-1.30, 1.24)	0.41 (-1.96, 1.25)	
log <i>Z_{SD}</i>	1.02 ± 0.75	-0.43 ± 1.02	0.32 ± 1.15	<0.001
	1.19 (-1.41, 2.01)	-0.58 (-1.96, 1.28)	0.79 (-1.96, 2.01)	
log <i>d</i>	0.22 ± 0.39	-0.04 ± 0.34	0.09 ± 0.39	<0.001
	0.32 (-0.54, 1.16)	-0.11 (-0.62, 0.59)	0.10 (-0.62, 1.16)	

Notes: The measured variables, *d*, *C*, *R_e*, *Z*, and *θ*, indicate thickness, capacitance, resistance, impedance magnitude, and phase angle, respectively. The transformed variables, *C_{SD}*, *R_{eSD}*, *Z_{SD}*, and *θ_{SD}*, signify standardized *C*, *R_e*, *Z*, and *θ* values, respectively. The transformed variables, log *d* and log *Z_{SD}* denote logarithmized *d* value and standardized logarithmized *Z* value. The listed values were mean ± standard deviation (SD) on the upper row and median (range) on the lower one. All *p*-values of group comparisons are obtained by fitting univariate logistic regression models with the generalized estimating equations (GEE) method to account for the correlations between repeated measurements.

doi:10.1371/journal.pone.0093647.t001

indices include capacitance (*C*), resistance (*R_e*), impedance magnitude (*Z*), and phase angle (*θ*). Additionally, the thickness (*d*) of the sample was measured by vernier caliper. Temperature and relative humidity were recorded.

Statistics analysis

Statistical analysis of the electrical impedance system was performed using the R 3.0.2 software (R Foundation for Statistical Computing, Vienna, Austria) [23]. In statistical testing, two-sided *p* value ≤ 0.05 was considered statistically significant. To compare the differentiating powers across frequencies, all observations from 10 frequencies were standardized and examined by conditional plots. After scrutinizing the differences in the conditional plots at 10 frequencies, and also referring to previous studies about keratinized tissues [4], we chose 80 Hz as the optimal frequency due to its differentiating capability (Text S1). For univariate analysis, the measured indices, *d*, *C*, *R_e*, *Z*, and *θ*, at 80 Hz were standardized and/or logarithmized to be log *d*, *C_{SD}*, *R_{eSD}*, *Z_{SD}*, log *Z_{SD}* and *θ_{SD}*, respectively. The distributional properties of these continuous variables were expressed by mean ± standard

deviation (SD). These indices were then analyzed by fitting univariate logistic regression model with the generalized estimating equations (GEE) method for examination on the discrimination abilities between clavus and verruca data. Note that the use of the GEE method was to account for the correlations between the repeated measurements within subjects on the lesions.

To generate a best model with predictive factors, multivariate analysis was further performed by fitting multivariate logistic regression model with the same GEE method. The two indices, log *Z_{SD}* and *θ_{SD}*, were identified as predictive factors by a stepwise variable selection procedure. To validate the model, the basic model-fitting techniques were applied for (1) variable selection, (2) goodness-of-fit (GOF) assessment, and (3) regression diagnostics and remedies. The GOF assessments the estimated area under the receiver operating characteristic (ROC) curve, adjusted generalized *R*², and the Hosmer-Lemeshow GOF test. In practice, the value of the *c* statistic (0 ≤ *c* ≤ 1) ≥ 0.7 suggests an acceptable level of discrimination power. Adjusted generalized *R*² ≥ 0.30 indicates an acceptable fit of a logistic regression model. And, larger *p* values of the Hosmer-Lemeshow GOF test indicate better fits. As regards to

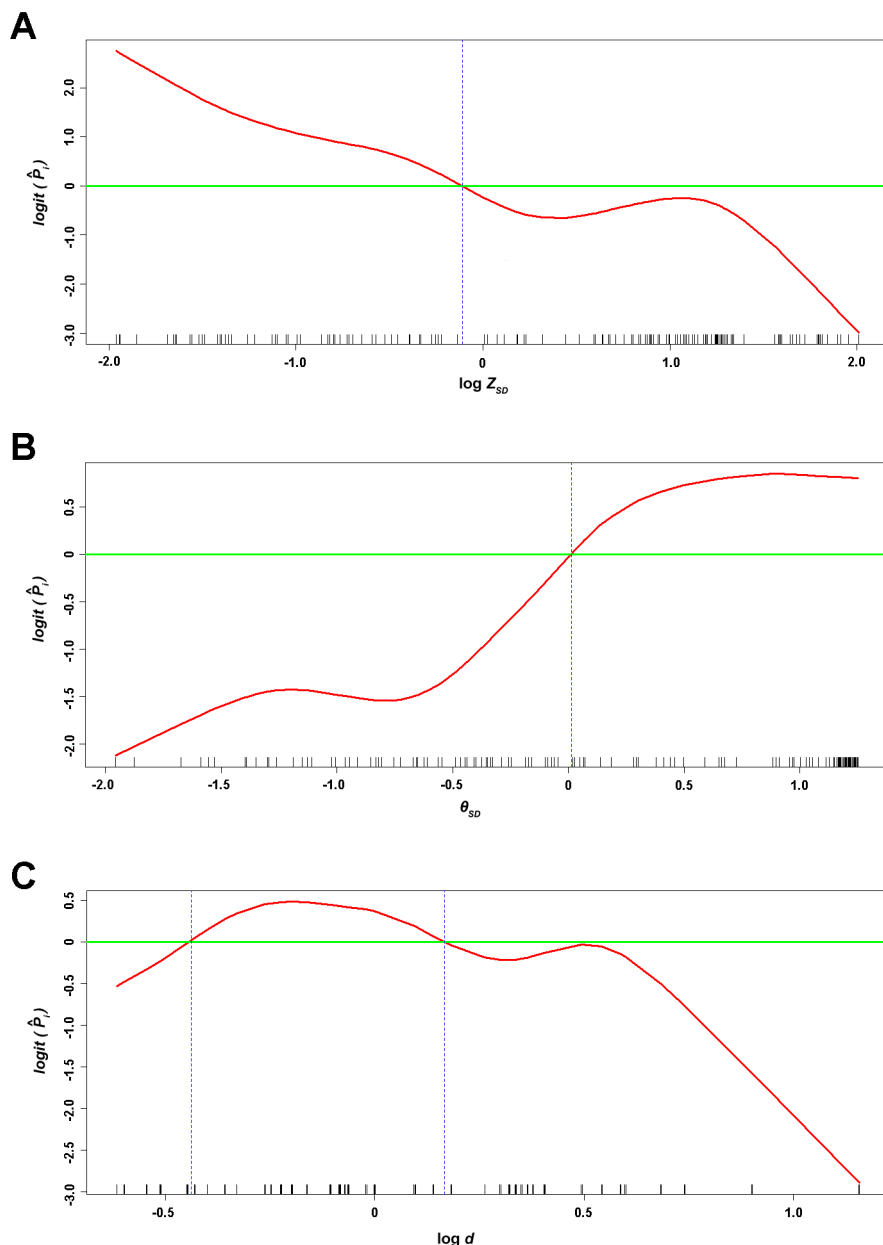


Figure 2. The GAM plots of the predictors, $\log Z_{SD}$ (A), θ_{SD} (B), and $\log d$ (C) respectively. The generalized additive models plots reveal the smoothed partial effects of the predictors in modeling the probability of being verruca. The distribution of the observed values of $\log Z_{SD}$, θ_{SD} , and $\log d$ are shown by the rugs on the X-axes. The Y-axes are the logit of the estimated probability of being verruca (\hat{P}_i), i.e., $\log\left(\frac{\hat{P}_i}{1-\hat{P}_i}\right)$. The horizontal green line indicates the place where $\hat{P}_i = 0.5$.
doi:10.1371/journal.pone.0093647.g002

regression diagnostics, the non-linear effects of continuous covariates were detected by the generalized additive models (GAM), such that faults in the model can be exposed.

Results

To discriminate the electrical properties between clavus and verruca, the measured and transformed indices of clavus at 80 Hz are compared with those of verruca in Table 1. For statistical analysis, 87 clavus and 84 verruca observations were used. By fitting univariate logistic regression analysis with the GEE method, all impedance indices are significantly different between clavus and verruca ($p < 0.001$), except C and C_{SD} . In Figure 1, the

conditional box plots of the measured indices further demonstrate that the absolute value of θ index of clavus is higher than that of verruca. Moreover, R_e and ζ values of clavus are approximately ten times higher than those of verruca. These results indicate that high impedance is associated with clavus, whereas low impedance in verruca. Moreover, R_e and ζ indices can be used to best distinguish clavus and verruca.

To generate a model for estimating the probability of being verruca versus clavus, all the indices, are analyzed using multivariate logistic regression with the GEE method. Moreover, the GAM plots of Figures 2A and 2B depict the approximately linear partial effects of predictors, $\log Z_{SD}$ and θ_{SD} , for the

Table 2. Multivariate analysis of the predictors of verruca at 80 Hz by fitting multiple logistic regression model with the generalized estimating equations (GEE) method.

Covariate	Estimate regression coefficient	Robust Standard Error	Chi-Square test	p Value	Estimated Odds Ratio	95% Confidence Interval of Odds Ratio
Intercept	-0.0198	0.5613	0.0012	0.9719	-	-
$\log Z_{SD}$	-0.9008	0.5670	2.5245	0.1121	0.406	0.134-1.234
θ_{SD}	0.8347	0.7112	1.3773	0.2406	2.304	0.572-9.288

Goodness-of-fit assessment: Number of clusters = 57, number of observations = 166, the estimated area under the Receiver Operating Characteristic (ROC) curve = 0.875 > 0.7, adjusted generalized $R^2 = 0.512 > 0.3$, and Hosmer-Lemeshow goodness-of-fit F test $p = 0.350 > 0.05$ ($df = 9, 156$).

Prediction: To calculate the estimated probability of being verruca (i.e., the predicted value, \hat{P}_i) given the observed covariate values, one can use the following formula. According to the above fitted multiple logistic regression model

$$\text{logit}(\hat{P}_i) = \log\left(\frac{\hat{P}_i}{1-\hat{P}_i}\right) = -0.0198 - 0.9008 \times \log Z_{SD} + 0.8347 \times \theta_{SD} \text{ the predicted value of observation } i \text{ is}$$

$$\hat{P}_i = \frac{1}{1 + \exp[-(-0.0198 - 0.9008 \times \log Z_{SD} + 0.8347 \times \theta_{SD})]} \text{ where } \log Z_{SD} = \text{logarithmized standardized } Z \text{ value, and } \theta_{SD} = \text{standardized } \theta \text{ value.}$$

doi:10.1371/journal.pone.0093647.t002

probability of being verruca respectively, but Figure 2C reveals an apparently nonlinear partial effect of $\log d$ and identified two appropriate cut-off points in discretizing. Therefore, one of the best models is selected (Text S2). In the final model, the estimated odds ratios (ORs) of predictors, $\log Z_{SD}$ and θ_{SD} , are 0.406 ($p = 0.1121$) and 2.304 ($p = 0.2406$), respectively (Table 2). The probability of being verruca (i.e., the predicted value) can be estimated by

$$\hat{P}_i = \frac{1}{1 + \exp(0.0198 + 0.9008 \times \log Z_{SD} - 0.8347 \times \theta_{SD})}$$

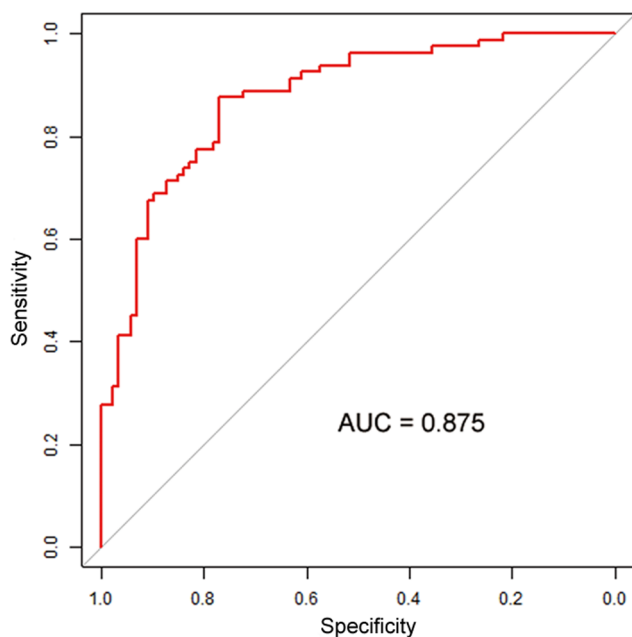


Figure 3. The Receiver Operating Characteristic (ROC) curve for the prediction of verruca. The estimated area under the ROC curve (AUC) is 0.875.

doi:10.1371/journal.pone.0093647.g003

As \hat{P}_i value approaches 1, the more probable the sample is associated with verruca. If \hat{P}_i value approaches 0, the more likely the sample is clavus. Furthermore, based on the above model, GOF assessment is used to validate the performance of the model. The area under the ROC is 0.875 (>0.7) (Figure 3), the adjusted generalized R^2 is 0.512 (>0.3), and the p value of the Hosmer-Lemeshow GOF test is 0.350 (>0.05). These results all pass the tests for best model-fitting techniques. Overall, a model with $\log Z_{SD}$ and θ_{SD} as predictive factors is generated for differentiating verruca from clavus, and the validity of the model is determined by GOF method.

Discussion

Impedance is proposed in this study to reflect the different histological constituents of clavus and verruca, so as to assemble a new electrical impedance system for differentiating these two lesion types. Research have disclosed that the impedance/resistivity of stratum corneum is greater than those of other tissues in the human body [24,25], whereas hydration of intact skin decreases the impedance [10,11]. In other words, impedance is high in stratum corneum and correlates reversely with the degree of hydration and admittance. Therefore, the relative high impedance values of clavus lesion found in the study may be resulted from its massive hyperkeratosis and relative thin, atrophic epidermis, which in turn point to the translucent central core under a dermoscope and biopsies. On the contrary, the components of verruca-relative thin stratum corneum, acanthosis proliferated by keratinocytes, and capillary proliferation-may explain why low impedance values are measured. Such differences in impedance values elucidate electrical impedance to be a competitive modality for discriminating the heterogeneous components of clavus from those of verruca.

To identify predictive factor from electrical impedance for model generation, this study discerns statistic differences between clavus and verruca, regarding resistance, impedance magnitude, phase angle, and thickness, but not capacitance. More importantly, resistance and impedance magnitude between clavus and verruca can differ by a factor of ten. However, only the model generated from the two parameters-impedance magnitude and phase angle-fits the data most. This can be explained by the following two equations [18]:

$$Z = \sqrt{R^2 + X^2}$$

$$\theta = \tan^{-1} \left(\frac{X}{R} \right)$$

Here, impedance is defined as total resistance of a biological conductor on alternating current. Simultaneously, it is comprised of two parts: one is resistance, and the other is reactance, defined as X . The reason why impedance magnitude and phase angle are the two parameters for model generation is clear. Furthermore, the advantage of using these two parameters is that they are transformed and calibrated values and as a result of that the predictive procedure becomes far less complicated. It is worthy to note that the use of these two indices in model design has been revealed in previous research, though relating neither to clavus nor to verruca. Impedance magnitude is found to be one of the important indices in analyzing electrical impedance spectra [6,10,12,18–20,26,27]. While, phase angle is in association with the studies concerning cancers, chronic obstructive pulmonary disease, HIV, hospital mortality of geriatric patients, and skin condition test [10,12,26,28,29].

After discussion on the three indices in question, attention is driven to the parameters, thickness and capacitance. Thickness parameter, although showing capabilities in distinguishing between clavus and verruca, is observed to pose problems in impedance analysis, due partly to the difficulties in specifying measured locations, and due partly to its variations caused by biological factors and environmental conditions [10,27]. In addition to this, the thickness of the sample, unlike all the other indices acquired by LCR-meter, is measured manually. Therefore, a model generated without thickness as predictor not only eliminates uncertainties embedded within, but also simplifies its procedure. As for capacitance, it is the only index derived from electrical impedance delivers otherwise result.

References

- Androphy EJ, Kimbauer R (2012). Human papilloma virus infections. In: Goldsmith LA, Katz SI, Gilchrist BA, Paller AS, Leffell DJ, Wolff K, editors. Fitzpatrick's Dermatology in General Medicine, 8th edition. McGraw-Hill Professional. pp. 2421–2433.
- DeLauro TM, DeLauro NM (2012). Corns and calluses. In: Goldsmith LA, Katz SI, Gilchrist BA, Paller AS, Leffell DJ, Wolff K, editors. Fitzpatrick's Dermatology in General Medicine, 8th edition. McGraw-Hill Professional. pp. 1111–1114.
- Johnsen GK, Martinsen OG, Grimnes S (2009). Estimation of *in vivo* water content of the stratum corneum from electrical measurements. *Open Biomed Eng J* 3: 8–12.
- Martinsen OG, Grimnes S, Sveen O (1997). Dielectric properties of some keratinized tissues. Part 1: Stratum corneum and nail in situ. *Med Biol Eng Comput* 35: 172–176.
- Yamamoto T, Yamamoto Y (1976). Electrical properties of the epidermal stratum corneum. *Med Biol Eng* 14: 151–158.
- Nicander I, Norlen L, Brockstedt U, Rozell BL, Forslind B, et al. (1998). Electrical impedance and other physical parameters as related to lipid content of human stratum corneum. *Skin Res Technol* 4: 213–221.
- Grimnes S (1983). Skin impedance and electro-osmosis in the human epidermis. *Med Biol Eng Comput* 21: 739–749.
- Martinsen OG, Grimnes S (2001). Facts and myths about electrical measurement of stratum corneum hydration state. *Dermatology* 202: 87–89.
- Lindholm-Sethson B, Han S, Ollmar S, Nicander I, Jonsson G, et al. (1998). Multivariate analysis of skin impedance data in long-term type 1 diabetic patients. *Chemometr Intell Lab Syst* 44: 381–394.
- Birgersson U, Birgersson E, Aberg P, Nicander I, Ollmar S (2011). Non-invasive bioimpedance of intact skin: mathematical modeling and experiments. *Physiol Meas* 32: 1–18.
- Curdy C, Naik A, Kalia YN, Alberti I, Guy RH (2004). Non-invasive assessment of the effect of formulation excipients on stratum corneum barrier function *in vivo*. *Int J Pharm* 271: 251–256.
- Nicander I, Nyren M, Emtestam L, Ollmar S (1997). Baseline electrical impedance measurements at various skin sites _ related to age and sex. *Skin Res Technol* 3: 252–258.
- Ollmar S, Nyren M, Nicander I, Emtestam L (1994). Electrical impedance compared with other non-invasive bioengineering techniques and visual scoring for detection of irritation in human skin. *Br J Dermatol* 130: 29–36.
- Nicander I, Ollmar S, Eek A, Lundh Rozell B, Emtestam L (1996). Correlation of impedance response patterns to histological findings in irritant skin reactions induced by various surfactants. *Br J Dermatol* 134: 221–228.
- Nyren M, Kuzmina N, Emtestam L (2003). Electrical impedance as a potential tool to distinguish between allergic and irritant contact dermatitis. *J Am Acad Dermatol* 48: 394–400.
- Glickman YA, Filo O, David M, Yayon A, Topaz M, et al. (2003). Electrical impedance scanning: a new approach to skin cancer diagnosis. *Skin Res Technol* 9: 262–268.
- Kuzmina N, Talme T, Lapins J, Emtestam L (2005). Non-invasive preoperative assessment of basal cell carcinoma of nodular and superficial types. *Skin Res Technol* 11: 196–200.
- Åberg P, Nicander I, Holmgren U, Geladi P, Ollmar S (2003). Assessment of skin lesions and skin cancer using simple electrical impedance indices. *Skin Res Technol* 9: 257–261.
- Beetner DG, Kapoor S, Manjunath S, Zhou X, Stoecker WV (2003). Differentiation among basal cell carcinoma, benign lesions, and normal skin using electric impedance. *IEEE Trans Biomed Eng* 50: 1020–1025.
- Aberg P, Nicander I, Hansson J, Geladi P, Holmgren U, et al. (2004). Skin cancer identification using multifrequency electrical impedance—a potential screening tool. *IEEE Trans Biomed Eng* 51: 2097–2102.

Last but not the least, the limitations of the model are detected by the GAM plots. Theoretically, the plots should be linear, but a partial linear is plotted. The non-linear effects of continuous covariates expose the inadequacies of the model. That is to say, misdiagnosis may occur, when lesions are not typical. Non-typical lesions include verruca with very thick corneal layer and few capillary proliferation, and clavus with exceeding hydration.

Conclusions

In conclusion, we employed electrical impedance as a novel tool to postulate a predictive model for differential diagnosis of clavus and verruca. From electrical impedance, $\log Z_{SD}$ and θ_{SD} , were two predictive factors derived for estimating the probability of being verruca versus clavus. Moreover, the validity of the model was approved by GOF and GAM methods. In spite of certain limitations, this study provides a rapid, low cost, safe and non-invasive alternative modality for physicians' clinic practice. Further application on *in vivo* diagnosis and investigation on circuit design for size reduction are expected.

Supporting Information

Figure S1 The stereoscopic features of (A) clavus and (B) verruca.

(PDF)

Text S1 Frequency selection.

(PDF)

Text S2 Final model selection.

(PDF)

Author Contributions

Conceived and designed the experiments: PLS FSJ. Performed the experiments: CYH PLS. Analyzed the data: CYH PLS SJC FSJ. Wrote the paper: CYH PLS SJC.

21. Emtestam L, Nicander I, Stenstrom M, Ollmar S (1998). Electrical impedance of nodular basal cell carcinoma: a pilot study. *Dermatology* 197: 313–316.
22. Dua R, Beetner DG, Stoecker WV, Wunsch DC (2004). Detection of basal cell carcinoma using electrical impedance and neural networks. *IEEE Trans Biomed Eng* 51: 66–71.
23. R Core Team (2010). *R: A Language and Environment for Statistical Computing*. Vienna, Austria: R Foundation for Statistical Computing.
24. Faes TJ, van der Meij HA, de Munck JC, Heethaar RM (1999). The electric resistivity of human tissues (100 Hz–10 MHz): a meta-analysis of review studies. *Physiol Meas* 20: R1–10.
25. Miklavčič D, Pavšelj N, Hart FX (2006). Electric properties of tissues. In: *Wiley Encyclopedia of Biomedical Engineering*, John Wiley & Sons, Inc., pp. 1–12.
26. M, Fischer H, Polat H, Helm EB, Frenz M, et al. (1995). Bioelectrical impedance analysis as a predictor of survival in patients with human immunodeficiency virus infection. *J Acquir Immune Defic Syndr Hum Retrovirol* 9: 20–25.
27. Mize MM, Aguirre Vila-Coro A, Prager TC (1989). The relationship between postnatal skin maturation and electrical skin impedance. *Arch Dermatol* 125: 647–650.
28. Gupta D, Lammersfeld CA, Burrows JL, Dahlk SL, Vashi PG, et al. (2004). Bioelectrical impedance phase angle in clinical practice: implications for prognosis in advanced colorectal cancer. *Am J Clin Nutr* 80: 1634–1638.
29. Wirth R, Volkert D, Rosler A, Sieber CC, Bauer JM (2010). Bioelectric impedance phase angle is associated with hospital mortality of geriatric patients. *Arch Gerontol Geriatr* 51: 290–294.